



SPECT Image Analysis Using Computational ROC Curve Based on Threshold Setup

Moo-Sub Kim*, Han-Back Shin*, Sunmi Kim*, Jae Goo Shim[†], Do-Kun Yoon*, Tae Suk Suh*

*Department of Biomedical Engineering and Research Institute of Biomedical Engineering, College of Medicine, The Catholic University of Korea, Seoul, [†]Department of Radiologic Technology Daegu Health College, Daegu, Korea

Received 21 July 2017
Revised 31 August 2017
Accepted 1 September 2017

Corresponding author

Tae Suk Suh
(suhsanta@catholic.ac.kr)
Tel: 82-2-2258-7232
Fax: 82-2-2258-7506

Co-corresponding author

Do-Kun Yoon
(dbsehrns@naver.com)
Tel: 82-2-2258-7504
Fax: 82-2-2258-7506

We proposed the objective ROC analysis method based on the setting of threshold value for evaluation of single photon emission computed tomography (SPECT) image. This proposed ROC analysis method uses the quantification computational threshold value to each signal on the SPECT image. The SPECT images for this study were acquired by using Monte Carlo n-particle extended simulation code (MCNPX, Ver. 2.6.0, Los Alamos National Laboratory, USA). The basic SPECT detectors and specific water phantom were realized in the simulation, and we could get the simulation results by the simulation operation. We tried to analyze the reconstructed images using threshold value application based objective ROC method. We can get the accuracy information of reconstructed region in the image. This proposed ROC technique can be helpful when we have to evaluate the weak signal for the NM image. In this study, the proposed threshold value based computational ROC analysis method can provide better objectivity than the conventional ROC analysis method.

Keywords: SPECT, Computational ROC, Threshold value, Objectivity

Introduction

Nuclear medicine (NM) images have been evaluated through a physical verification method such as modulation transfer function (MTF), root mean square (RMS), Winener spectrum, and entropy analysis, etc.¹⁻³⁾ However, these evaluation methods frequently caused some unexpected results which are different with an evaluation according to an observer. Although the number of data is same, the evaluation can be absolutely changed depending on the personal subjectivity with visual recognition ability and experience. In addition, because this subjective evaluation method is progressed without the objectivity, the correct evaluation of the image quality can be difficult. Thus, because the evaluation of NM image is easy to depend

on the observer's vision, the subjectivity based on the physical standard is required. Hawlet chart method, Landolt chart method, Burger's phantom, receiver operation characteristic (ROC) analysis have been used as the representative subjective evaluation method.^{4,5)} Although the ROC analysis based on signal detection is the subjective evaluation method of the observer, the observer's subjective decision can be considered as a quantitative factor.⁶⁻⁹⁾ The conventional ROC analysis method for the NM image is progressed by scoring the quality of the specific signal on the image, and the ROC curve can be made using both the sensitivity and the specificity, according to the score. And the image can be evaluated by comparing the area under the curve (AUC) value. For the score, when there are the signal and

the noise, if its response is 'Signal', it is denoted as 'true positive (TP)'. When there is the only noise, if its response is 'No Signal', it is denoted as 'true negative (TN)'. On the other hands, when there are the signal and the noise, if its response is 'No Signal', it is classified as 'false negative (FN)'. When there is the only noise, if its response is 'Signal', it is classified as 'false positive (FP)'. For these four classes, each score is assigned to draw the ROC curve. However, we proposed the objective ROC analysis method based on the setting of threshold value, for evaluation of single photon emission computed tomography (SPECT) image. This proposed ROC analysis method uses the quantification computational threshold value to each signal on the SPECT image.

Materials and Methods

The SPECT images for this study were acquired by using Monte Carlo n-particle extended simulation code (MCNPX, Ver. 2.6.0, Los Alamos National Laboratory, USA). The basic SPECT detectors and specific water phantom were realized in the simulation, and we could get the simulation results by the simulation operation. The specification of the detector and source definition is referred from the previous study.^{10,11} The water phantom which can emit the gamma ray of 662 keV (Cs-137) at the specific region was used to be scanned using SPECT in the simulation. This cylindrical water phantom (diameter=18 cm, height=6 cm, density=1 g/cm³) involved three radioisotope uptake regions (RURs). These three RURs (isotope content ratio=0.14%, 0.55%, 0.31%) took each different size (diameter=2 cm, 4 cm, and 3cm) and position ((-2.12, -3.00, -2.12), (0, -3.00, 2.00), and (2.12, -3.00, -2.12); the center of phantom=(0, 0, 0)). The lutetium yttrium oxyorthosilicate (LYSO, density=7.3 g/cm³) that is mainly used to detect gamma ray in the NM device was selected for the simulation. The size of detector was 28×28×3 cm³, and the parallel lead collimator (density=11.3 g/cm³) with 2 mm thickness, 20 cm height, and 69 frames was attached to the detector.¹² The projection numbers of the SPECT imaging in this study were 16, 32, 64, and 128 (due to 4 head SPECT modality). For each projection, the numbers of particle source (NPS) was set at 60 million. In addition, to reconstruct SPECT

image, graphics processing unit (GPU; NVIDIA GeForce GTX 770, 2 GB memory GDDR5 graphic card and compute unified device architecture (CUDA)) based ordered subset expectation maximization (OSEM) reconstruction algorithm was used using MATLAB (R2012a, Mathworks Inc., USA).

We tried to analyze the reconstructed images using threshold value application based objective ROC method. In order to progress this proposed evaluation method, the pixel address matching method is required. The pixel address matching method is similar to the image registration. However, it cannot be called as registration. The simple overlapping between the reconstructed image and the actual tomographic image such as the computed tomography (CT) image. The first process is the unification regarding both the pixel size and the matrix number. In spite of pixelated reconstructed image, we should divide the actual tomographic image as the pixel. Thus, we applied the grid pattern frame looks like the pixel to the actual tomographic image. And each pixel address value was assigned depending on the pixel's row-column. When the matrix size of two kinds of image was same, because each pixel address was same, we can match the address value between the reconstructed image and the actual tomographic image. Second, the setting of standard points for overlapping images was performed. We calculated there points from the reconstructed image and the actual tomographic image. At the actual tomographic image, the target's center points were measured. And then, the pixels including these points was found. In the case of the reconstructed image, the each pixel including the highest intensity from three RUR was found. Thus, we could overlap these two images.

We tried to include objective factor for drawing the ROC curve. At each pixel of reconstructed image matched with the actual tomographic image, when the specific pixel in the reconstructed image is involved on the part of the RUR at the actual tomographic image, Signal threshold value is applied to decide the TP (in case that the signal intensity level is over the 90%). And the signal threshold value can be adjusted according to the area ratio. Although the some pixel is located on the part of the RUR, if the signal intensity level is below the threshold, it is classified at the

FN. The FN case is remarkable mostly at the edge of the RUR. On the other hands, when the specific pixel in the reconstructed image is involved on the region without

RUR, Noise threshold value is applied to decide the TN (in case that noise intensity level is below 10%). Although some pixels are located at the out of RUR, if the noise

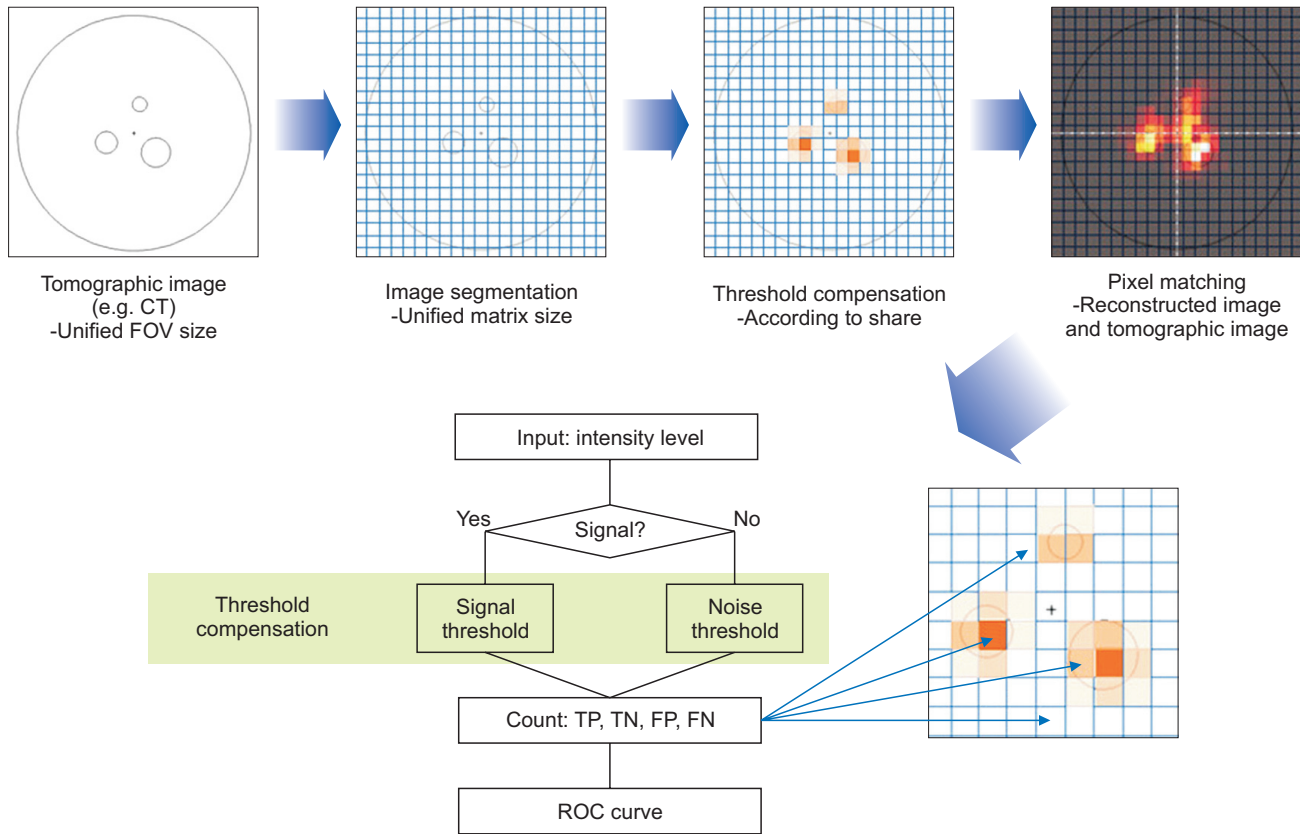


Fig. 1. Diagram of the threshold value based receiver operation characteristic (ROC) analysis method.

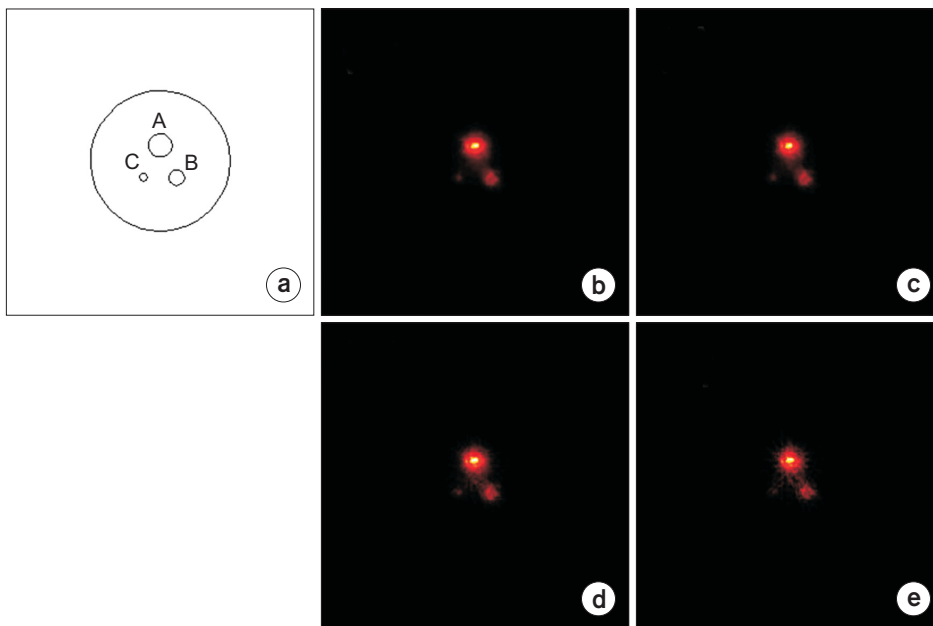


Fig. 2. Original water pattern of the single photon emission computed tomography (SPECT) phantom with three radioisotope uptake regions (RURs) (a). Reconstructed tomographic image using the graphic processing unit (GPU) based fast iterative reconstruction algorithm with (b) 128, (c) 64, (d) 32, and (e) 16 projections.

intensity level is over the threshold value, it is classified as the FP. Thus, we could get the four factors (TP, FN, TN, and FP) for drawing the ROC curve, and we could calculate the sensitivity and specificity using the many answers from the pixels (as matrix number; $N \times N$). Fig. 1 shows the method of threshold value based ROC analysis.

Results and Discussion

Fig. 2 shows the reconstructed images using the GPU

based OSEM reconstruction algorithm. The original pattern of water phantom including three RURs tagged as A, B, and C was shown at Fig. 2(a), and Fig. 2(b), (c), (d), and (e) show the reconstructed images using 128, 64, 32, and 16 projection data, respectively. Naturally, the more projection number made the better images. We can observe the three RURs clearly at (b), (c). However, in the case of region C in the (d) and (e), it is hard to identify region signal only using naked eyes. Because normal people is difficult to identify a blurred signal, this case can cause the confusing

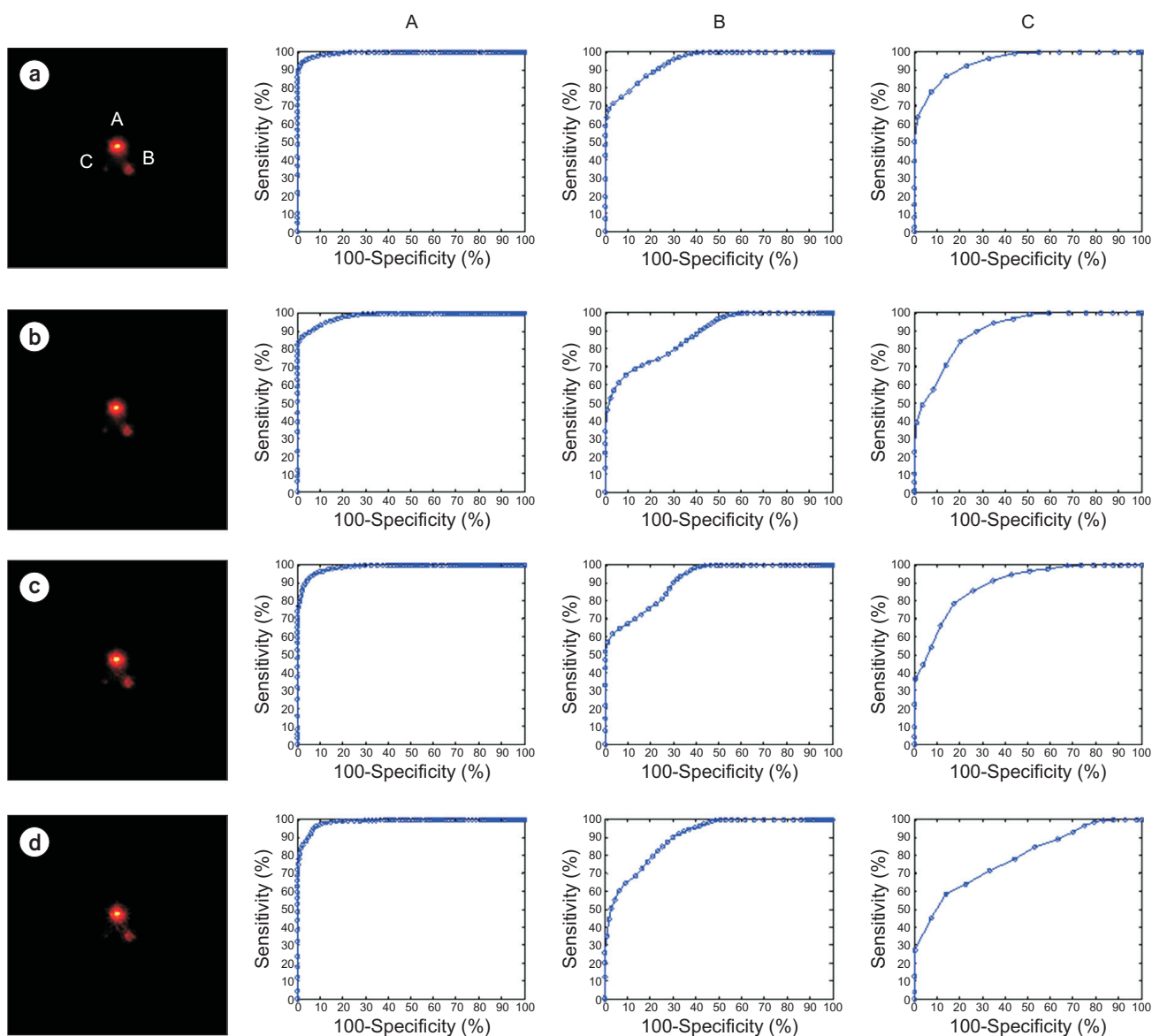


Fig. 3. Results of threshold value based receiver operation characteristic (ROC) analysis method for the reconstructed images. (a), (b), (c), and (d) is the reconstructed images using 128, 64, 32, and 16 projection data, respectively. A, B and C is the results the threshold value based ROC analysis method.

results regarding the conventional ROC analysis. Fig. 3(a)-(d) show the ROC curve results according to the 128, 64, 32, and 16 projection based reconstructed images, through the proposed threshold value based computational ROC technique. We acquired the AUC values from each ROC curve to compare the performance. The strong signal caused the good results about AUC value. This trend was noticeable at larger size signal, and greater projection number. Surely, if the signal is easy to be identified using the naked eyes, the ROC curve's pattern is close to ideal model. However, we focused on the weak signal case which is hard to be identified using only naked eyes. As a results, although the specific region regarding the weak signal is hard to be identified using only people's vision, the ROC curve was deducted ordinarily (region C in the (d) and (e)). In addition, we can get the accuracy information of reconstructed region in the image. This proposed ROC technique can be helpful when we have to evaluate the weak signal for the NM image. Moreover, if the image segmentation is progressed more minutely, we can acquire the better results. In addition, when we evaluate a specific image, the high level decision for both sensitivity and specificity, which are standards for verification, is ideal model as the ROC application. However, it is important that several conditions such as the disease and status, patient, etc. should be considered.

Conclusion

In this study, the proposed threshold value based computational ROC analysis method can provide better objectivity than the conventional ROC analysis method. When there is the weak signal which is hard to be identified using only naked eyes, the accuracy of reconstructed signal in the NM image can be calculated. In the future, we will applied this technique at the PET image as well as more SPECT images case.

Conflicts of Interest

The authors have nothing to disclose.

Availability of Data and Materials

All relevant data are within the paper and its Supporting Information files.

References

1. R. B. Mazess, H. M. Wahner, Nuclear medicine and densitometry. Osteoporosis 1988.
2. J. J. Conway, M. Maizels, The "well tempered" diuretic renogram: a standard method to examine the asymptomatic neonate with hydronephrosis or hydroureteronephrosis. A report from combined meetings of The Society for Fetal Urology and members of The Pediatric Nuclear Medicine Council--The Society of Nuclear Medicine. Journal of nuclear medicine: official publication, Society of Nuclear Medicine 1992;33:2047-2051.
3. C. Gabriela, M. Chianelli, A. Signore, Nuclear medicine imaging of diabetic foot infection: results of meta-analysis. Nuclear medicine communications 2006;27:757-764.
4. H. Kitagawa, A. G. Farman, M. Wakoh, et al. Objective and subjective assessments of Kodak Ektaspeed plus new dental X-ray film: a comparison with other conventional X-ray films. The Bulletin of Tokyo Dental College 1955;36:61-67.
5. Y. Ojima, A. Tsujikawa, M. Hangai, et al. Retinal sensitivity measured with the micro perimeter 1 after resolution of central serous chorioretinopathy. American journal of ophthalmology 2008;146:77-84.
6. J. Eng, Receiver operating characteristic analysis. Academic radiology 2005;12:909-916.
7. M. Greiner, P. Dirk, R. D. Smith, Principles and practical application of the receiver-operating characteristic analysis for diagnostic tests. Preventive veterinary medicine 200;45:23-41.
8. K. H. Zou, A. J. O'Malley, L. Mauri, Receiver-operating characteristic analysis for evaluating diagnostic tests and predictive models. Circulation 2007;115:654-657.
9. A. T. Peterson, M. Papeş, J. Soberón, Rethinking receiver operating characteristic analysis applications in ecological niche modeling. Ecological modelling 2008;213:63-72.
10. Yoon DK, Jung JY, Jo Hong K, et al. GPU-based prompt gamma ray imaging from boron neutron capture therapy. Medical physics 2015;42:165-169.

11. Yoon D-K, Jung J-Y, Jo Hong K, et al. Tomographic image of prompt gamma ray from boron neutron capture therapy: A Monte Carlo simulation study. *Applied Physics Letters* 2014;104:083521.
12. Shin HB, Yoon DK, Jung JY, et al. Prompt gamma ray imaging for verification of proton boron fusion therapy: A Monte Carlo study. *Physica medica* 2016;32:1271-1275.